Cell and Tissue Research (2020) 380:615–625
https://doi.org/10.1007/s00441-019-03165-w

REGULAR ARTICLE

Foxn1 and *Prkdc* genes are important for testis function: evidence from nude and scid adult mice

Carolina FA Oliveira[1] · Nathália LM Lara[1] · Samyra MSN Lacerda[1] · Rodrigo R Resende[2] · Luiz R França[1] · Gleide F Avelar[1]

Received: 31 May 2019 / Accepted: 19 December 2019 / Published online: 16 January 2020
© Springer-Verlag GmbH Germany, part of Springer Nature 2020

Abstract

Mutations in *Foxn1* and *Prkdc* genes lead to nude and severe combined immunodeficiency (scid) phenotypes, respectively. Besides being immunodeficient, previous reports have shown that nude mice have lower gonadotropins and testosterone levels, while scid mice present increased pachytene spermatocyte (PS) apoptosis. Therefore, these specific features make them important experimental models for understanding *Foxn1* and *Prkdc* roles in reproduction. Hence, we conducted an investigation of the testicular function in nude and scid BALB/c adult male mice and significant differences were observed, especially in Leydig cell (LC) parameters. Although the differences were more pronounced in nude mice, both immunodeficient strains presented a larger number of LC, whereas its cellular volume was smaller in comparison to the wild type. Besides these alterations in LC, we also observed differences in androgen receptor and steroidogenic enzyme expression in nude and scid mice, suggesting the importance of *Foxn1* and *Prkdc* genes in androgen synthesis. Specifically in scid mice, we found a smaller meiotic index, which represents the number of round spermatids per PS, indicating a greater cell loss during meiosis, as previously described in the literature. In addition and for the first time, Foxn1 was identified in the testis, being expressed in LC, whereas DNA-PKc (the protein produced by *Prkdc*) was observed in LC and Sertoli cells. Taken together, our results show that the changes in LC composition added to the higher expression of steroidogenesis-related genes in nude mice and imply that Foxn1 transcription factor may be associated to androgen production regulation, while *Prkdc* expression is also important for the meiotic process.

Keywords Nude mice · Scid mice · Leydig cell · *Foxn1* · *Prkdc*

Introduction

A recessive autosomal mutation in the *Foxn1* gene ($Foxn1^{-/-}$) leads to the nude mouse phenotype, characterized by a lack of skin fur development and agenesis of the thymus (Mecklenburg et al. 2005). The *Foxn1* gene encodes a transcription factor (Foxn1) from the winged helix/forkhead family (Byrd 1993; Nehls et al. 1994) that consists of over 100 proteins, several of which are reported to regulate reproduction (Uhlenhaut and Treier 2011) and gonadotropin (follicle-stimulating hormone (FSH) and luteinizing hormone (LH)) gene expression (Thackray 2014). Foxl2, for instance, has a central role in female sex determination and is required for normal *Fshb* expression (Justice et al. 2011). Moreover, Foxo1 is important for spermatogonial stem cell self-renewal and modulates gonadotropin beta-subunit gene expression (Goertz et al. 2011; Skarra et al. 2013), while Foxp3 is relevant for spermatogenesis and male fertility (Jasurda et al. 2014). Even though the studies regarding testis function in nude mice are scarce, it is known that they have lower serum levels of testosterone and gonadotropins in comparison to the wild type (Rebar et al. 1982). Therefore, as other proteins of the family, Foxn1 might have a potential role in hormonal regulation and reproduction.

Mutations in the *Prkdc* gene lead to the severe combined immunodeficiency (scid) phenotype. The DNA-dependent protein kinase (DNA-PK) is an enzyme important for repairing DNA double-strand breaks. This enzyme comprises two subunits: one is the catalytic (DNA-PKc), encoded by the *Prkdc* gene, while the other is the heterodimer Ku70/80,

✉ Gleide F Avelar
gleideav@yahoo.com.br

[1] Laboratory of Cellular Biology, Department of Morphology, Federal University of Minas Gerais, Belo Horizonte, MG, Brazil

[2] Department of Biochemistry and Immunology, Federal University of Minas Gerais, Belo Horizonte, MG, Brazil

responsible for DNA recognition (Lees-Miller and Meek 2003). Despite being considered fertile, Hamer et al. (2003) observed that scid male mice have an increase of pachytene spermatocyte apoptosis at stage IV of the seminiferous epithelium cycle (SEC), when there is a meiotic checkpoint. Therefore, the susceptibility of this cell type to apoptosis is related to a failure in repairing DNA double-strand breaks that occur during genetic recombination (Hamer et al. 2003; De Rooij and De Boer 2003).

Due to their peculiar reproductive aspects, both nude and scid mice are potential experimental models for the understanding of *Foxn1* and *Prkdc* gene roles in reproduction. Therefore, the aim of the present study is to perform a detailed investigation of testicular function in nude and scid mice, seeking to provide further insights into the importance of these genes in the regulation of spermatogenesis.

Material and methods

Animals, testis sample collection and processing

The nude mice used in this study were purchased from Taconic, Germantown, USA and the scid mice from Fiocruz, Bahia, Brazil. Sixteen sexually mature (70 days) male mice, from each of the investigated strains (BALB/c wild type, BALB/c nude and BALB/c scid), were used in the following distribution for each group: nine animals were used for light microscopy and histomorphometry, four were used for immunohistochemistry and three had their testis collected for qPCR gene expression analyses. The wild-type mice were housed in a standard animal facility and the immunodeficient mice were housed in filtered microisolator cages, with a ventilated rack system (Alesco®), under a controlled photoperiod (12 h light, 12 h dark), with access to autoclaved water and rodent food ad libitum.

In accordance with the animal experimentation guidelines, in the present study, we sought to use the minimum necessary number of animals to obtain a biological response. Therefore, by determining the sample size based on the most instable variable that was established as the Leydig cell number per gram of testis (Auharek et al. 2011), the experimental number of animals needed was obtained from a calculation made according to Sampaio (2002). Hence, our histomorphometric analysis was statistically validated using nine animals per group.

The mice used for histomorphometry ($n = 9$ per group) and immunohistochemistry ($n = 4$ per group) were weighed, anesthetized with an intraperitoneal injection of pentobarbital (150 mg/kg, Thiopentax®; Cristalia, Brazil) and perfusion-fixed with glutaraldehyde 4% in 0.05 M phosphate buffer (for histomorphometric analysis) or Bouin's solution (for immunohistochemistry), following the procedure described by Sprando et al. (1990). After fixation, testes were weighed and sectioned in smaller fragments with a razor blade. The testis fragments were dehydrated in increasing alcohol concentrations and embedded in glycol methacrylate (Leica Biosystems, Germany) for histomorphometric analysis or Paraplast® (Sigma-Aldrich, Germany) for immunohistochemistry.

For the gene expression analysis, the mice ($n = 3$ per group) were weighed, euthanized and orchiectomized; had their testis frozen in liquid nitrogen; and were stored at − 80 °C. The messenger RNA (mRNA) relative levels of androgen receptor, 3-beta-hydroxysteroid dehydrogenase (3BHSD) and aromatase were analyzed. Beta-actin expression was used as an internal control.

Histomorphometric analysis

Seminiferous tubular diameter and height of the seminiferous epithelium were measured from 20 tubules per animal at 400x magnification using an ocular micrometer calibrated with a stage micrometer. The volume densities of testis tissue components were determined from 15 randomly chosen fields per animal using a 441-point intersection grid placed in the eyepiece of a light microscope (6615 points) at 400x magnification. Points were classified as one of the following: seminiferous tubules (comprising tunica propria, seminiferous epithelium and lumen), Leydig cells, connective tissue, blood and lymphatic vessels. The volume of each testis component was determined as the product of its volume density and testis volume (the testis capsule was excluded from the testis weight). The total length of the seminiferous tubule was obtained by dividing the seminiferous tubule volume by the square radius of the tubule times π (Attal and Courot 1963; Dorst and Sajonski 1974).

For the cell counts, spermatogonia, pre-leptotene/leptotene spermatocytes, pachytene spermatocytes, round spermatids and Sertoli cell (SC) nucleoli present at stage VII of the seminiferous epithelium cycle were counted in 10 round or nearly round seminiferous tubule cross-sections, chosen at random, for each animal. These counts were corrected for section thickness (4 μm) and nuclear or nucleolar diameter according to Abercrombie (1946), as modified by Amann and Almquist (1962). For this purpose, the diameters of 10 nuclei or nucleoli were measured per animal for each cell type analyzed. Cell ratios were obtained from the corrected counts obtained at stage VII. The total number of SC was determined from the corrected counts of SC nucleoli per seminiferous tubule cross-section and the total length of seminiferous tubules according to Hochereau-de Reviers and Lincoln (1978). Daily sperm production (spermatogenic efficiency) was determined according to the formula developed by Franca (1992), as follows: DSP = total number of SC per testis × ratio of round spermatids to SC at stage VII × stage VII relative frequency (%) / stage VII duration (days).

Regarding Leydig cells (LC), as their nucleus in mice is round or nearly round, the nuclear volume was easily determined from its mean nuclear diameter. For this purpose, 30 nuclei showing an evident nucleolus were measured for each animal. LC nuclear volume was obtained by the formula 4 / 3πr3, where r is nuclear diameter / 2. To calculate the proportion between nucleus and cytoplasm and the cytoplasmic volume, a 441-point intersection grid was placed over the sectioned material at × 1000 magnification and one thousand points over LC per testis were counted for each animal. The volume of each individual LC was obtained as the sum of its nuclear and cytoplasmic volumes. The number of LC per testis was estimated from the LC individual volume and the volume density occupied by LC in the testis parenchyma.

Quantitative qPCR gene expression

The primers sequences chosen for the testicular mRNA relative level analysis (Table 1) were obtained from validated sequences at the PrimerBank (http://pga.mgh.harvard.edu/primerbank) and synthetized by Integrated DNA Technologies (IDT®). Total RNA was extracted using TRIzol® (Thermo Fisher Scientific, USA) according to the manufacturer's instructions and its concentration was determined by spectrophotometry in NanoDrop 2000 (NanoDrop Inc., Wilmington, DE, USA). After that, the volume corresponding to 2 μg of RNA was subjected to reverse transcription followed by a polymerase chain reaction. Using the cDNA generated, the qPCR was performed using SYBR Green Supermix 240 (Bio-Rad, Marnes la Coquette, France) and each assay was replicated with the same parameters. Data were normalized to beta actin, as a reference gene, which showed a constant expression pattern under the conditions analyzed. All procedures were carried out as described by Morais et al. (2017).

Table 1 Primers used for gene expression

Primer	Sequence
Androgen receptor forward	5′-CTGGGAAGGGTCTACCCAC-3′
Androgen receptor reverse	5′-GGTGCTATGTTAGCGGCCTC-3′
Aromatase forward	5′-ATGTTCTTGGAAATGCTGAA CCC-3′
Aromatase reverse	5′-AGGACCTGGTATTGAAGACGAG-3′
3-Beta-HSD forward	5′-TGGACAAAGTATTCCGACCAGA-3′
3-Beta-HSD reverse	5′-GGCACACTTGCTTGAACACAG-3′
Beta-actin forward	5′-GGCTGTATTCCCCTCCATCG-3′
Beta-actin reverse	5′-CCAGTTGGTAACAATGCCATGT-3′

Immunohistochemistry

For the immunohistochemistry analyses, the procedures were as follows: testis sections were mounted on coated slides, dewaxed and rehydrated in decreasing alcohol concentrations. Then, antigen retrieval was performed in citrate buffer (pH 6.0) for 5 min after boiling in a microwave oven. Slides were incubated in 30% hydrogen peroxide (Sigma-Aldrich) to block endogenous peroxidase activity. Nonspecific binding sites were blocked with 10% normal serum for 30 min, before the addition of primary antibodies and incubation overnight at 4 °C. After this procedure, the slides were exposed to the appropriate secondary antibodies for 60 min at room temperature. Detection of the signal was performed by incubating the sections in streptavidin (TS-125-HR, Thermo Scientific) for 30 min, followed by a reaction with peroxidase substrate 3,3-diaminobenzidine (DAB) (Sigma-Aldrich) and counterstaining with hematoxylin (Merck).

We used primary antibodies against androgen receptor (1:150, cat no. SC-815; Santa Cruz Biotechnology, USA), the steroidogenic enzyme aromatase (1:300, cat no. PA5-19633; Thermo Fisher Scientific, UK) and 3BHSD (1:750, cat no. SC-30820; Santa Cruz Biotechnology, USA), as well as antibodies anti-Foxn1 (1:400, cat no. SC-30195; Santa Cruz Biotechnology, USA) and anti-DNA-PKc (1:250, cat no. SC-9051; Santa Cruz Biotechnology, USA). The slides were qualitatively analyzed in order to evaluate which cell types were labeled as well as their location in the testicular parenchyma.

In order to better evaluate the expression of the androgen receptor, aromatase and 3BHSD, we decided to perform a second method of analysis. Thus, in addition to mRNA quantification by qPCR, we also performed a semiquantitative analysis of the intensity of labeling obtained for those proteins assessed through immunohistochemistry, as previously described elsewhere (Dornas et al. 2007, 2008; Oliveira et al. 2013). For this analysis, six random images were captured from the testicular parenchyma of each animal using an Olympus BX60 microscope with a coupled camera. The images were treated to convert to gray scale in Photoshop CS3 v10.0 and the pixel intensity was measured from 30 to 60 labeled cells per animal using ImageJ 1.47t, normalized by the pixel intensity obtained in the background of the image (lumen of seminiferous tubules or blood vessels).

Statistical analysis

Values are expressed as mean ± standard error of the mean (SEM) and were tested for normality and homoscedasticity of the variances. Data were analyzed accordingly using ANOVA and the means were compared using the Student-Newman-Keuls test. Pearson's correlation was used to evaluate the relationship between two variables. All analyses were performed using GraphPad Prism 6 (GraphPad Software, Inc.) and the significance level considered was $p < 0.05$.

Results

Biometric data

The body and testicular weights and gonadosomatic index are shown in Table 2. No difference was observed in the body weight among the three groups. On the other hand, in comparison to the wild type, the testis weight and gonadosomatic index (ratio between total testis mass and body mass) were significantly smaller in the nude mice.

Histomorphometric analysis

As observed in Table 2, although the tubular diameter and seminiferous epithelium height were higher in the nude mice in comparison to the other groups, the total length of seminiferous tubules per testis was significantly smaller in this strain.

The volume density (%) and absolute volume (μl) of each testicular component are summarized in Table 3. The intertubular compartment and LC volume densities were different among the three groups and higher values were observed in the immunodeficient strains, particularly for the scid mice. Because the higher values were found for the scid mice intertubular compartment and LC, this pattern was also followed for absolute volumes. Therefore, a positive and significant correlation between intertubular compartment and LC occupancy was found for nude ($r = 0.82$) and scid ($r = 0.91$) mice. Additionally, significant differences were observed for blood vessels, lymphatic space and connective tissue occupancies. The absolute volume and the percentage of blood vessels were significantly reduced, while connective tissue volume density and the absolute volume were significantly increased in scid mice, when compared to the other groups. The lymphatic space volume density, as well as the absolute volume, were smaller in nude mice and showed an intermediate value in scid mice when compared to the wild type. On the other hand, as expected, the tubular compartment volume density and the absolute volume showed an opposite pattern when compared to the intertubular space, and the smallest values were found for the immunodeficient strains. In the tubular compartment, significant differences were observed for lumen and tunica propria absolute volumes and the volume densities. Hence, when compared to the wild type, the smallest lumen occupancy was observed for scid mice, while nude mice presented an intermediate value. An opposite pattern was found for tunica propria, once the highest value was found for scid mice.

Cell counts

The cell counts and ratios obtained at stage VII of the seminiferous epithelium cycle are shown in Table 4. The lowest SC efficiency was observed in scid mice, with approximately 8 round spermatids supported by each SC. The meiotic index, which expresses the number of round spermatids produced per pachytene spermatocyte and represents the cell loss during meiosis, was lower for scid, in comparison with nude and wild-type mice.

Still focusing on SC, its numbers per testis and per gram of testis were significantly higher in the scid mice than in the other two strains. Furthermore, as shown in Table 4, daily sperm production per testis was significantly smaller in nude mice, whereas this parameter per gram of testis was higher in the scid mice. Therefore, as expected, daily sperm production per testis showed a positive and significant correlation with the SC number per testis in wild-type, nude and scid strains ($r = 0.84$, $r = 0.86$ and $r = 0.73$, respectively).

Substantial differences were observed in the LC parameters (Table 5). In this regard, the nuclear, cytoplasmic and individual volumes of LC in nude mice were the lowest volumes found in this study. Interestingly, the number of LC per testis and per gram of testis were also significantly different among the strains investigated, showing an opposite trend when compared to the cellular volume. In this regard, LC number was

Table 2 Biometric and morphometric data in BALB/c wild-type, nude and scid mice (mean ± SEM)

	Wild type	Nude	scid
Body weight (g)	26 ± 0.5	28 ± 0.8	25 ± 1
Testis weight (mg)	102 ± 2^{a}	83 ± 5^{b}	89 ± 6^{ab}
Gonadosomatic index (%)	0.8 ± 0.02^{a}	0.6 ± 0.03^{b}	0.7 ± 0.03^{a}
Tubular diameter (μm)	224 ± 2^{a}	243 ± 3^{b}	212 ± 3^{c}
Seminiferous epithelium height (μm)	77 ± 1^{a}	84 ± 2^{b}	76 ± 1^{a}
TLST/testis (m)	2.3 ± 0.07^{a}	1.5 ± 0.09^{b}	2.1 ± 0.15^{a}
TLST/testis g (m)	23 ± 0.4^{a}	19 ± 0.4^{b}	25 ± 0.6^{c}

Different letters in the same line indicate significant differences ($p < 0.05$) among groups

TLST total length of seminiferous tubules

Table 3 Volume density (%) and absolute volumes (μl) of testis components in BALB/C wild type, nude and scid mice (mean ± SEM)

	Wild type Volume density % (μl)	Nude	scid
Seminiferous tubules	92 ± 0.004^{a} (91 ± 2)^{a}	90 ± 0.01^{b} (72 ± 5)^{b}	88 ± 0.01^{c} (76 ± 6)^{b}
Seminiferous epithelium	80 ± 0.01 (79 ± 2)^{a}	78 ± 0.005 (62 ± 4)^{b}	78 ± 0.01 (67 ± 6)^{ab}
Lumen	9.4 ± 0.01^{a} (9.3 ± 0.8)^{a}	7.5 ± 0.005^{b} (6 ± 0.6)^{b}	4.1 ± 0.001^{c} (3.5 ± 0.3)^{c}
Tunica propria	3 ± 0.001^{a} (2.9 ± 0.1)^{a}	4.5 ± 0.002^{b} (3.5 ± 0.2)^{a}	6.2 ± 0.004^{c} (5.3 ± 0.6)^{b}
Intertubular compartment	8 ± 0.004^{a} (7.8 ± 0.4)^{a}	10 ± 0.01^{b} (7.9 ± 0.5)^{a}	12 ± 0.01^{c} (10.2 ± 0.5)^{b}
Leydig cells	4 ± 0.004^{a} (3.9 ± 0.4)^{a}	7 ± 0.006^{b} (5.6 ± 0.6)^{b}	9 ± 0.01^{c} (7.3 ± 0.3)^{c}
Blood vessels	2.6 ± 0.003^{a} (2.5 ± 0.3)^{a}	2.6 ± 0.004^{a} (2 ± 0.3)^{a}	1.5 ± 0.002^{b} (1.2 ± 0.2)^{b}
Lymphatic space	0.93 ± 0.001^{a} (0.9 ± 0.1)^{a}	0.13 ± 0.0004^{b} (0.1 ± 0.03)^{b}	0.45 ± 0.001^{c} (0.4 ± 0.1)^{c}
Connective tissue	0.5 ± 0.0003^{a} (0.5 ± 0.04)^{a}	0.3 ± 0.001^{a} (0.2 ± 0.08)^{a}	1.5 ± 0.002^{b} (1.3 ± 0.2)^{b}

Different letters in the same line represent significant statistical difference ($p < 0.05$)

highly increased in nude mice in comparison with the other two groups.

Immunohistochemistry and qPCR gene expression

The protein localization, pixel intensity quantification and relative gene expression levels of the androgen receptor, 3BHSD and aromatase are shown in Figs. 1, 2, and 3, respectively. In general, the results from qPCR and pixel intensity measurement followed a similar pattern. As expected, androgen receptor expression was restricted to the nuclear compartment of the peritubular myoid cell, endothelial cell, SC and LC (Fig. 1). The pixel intensity analysis showed stronger labeling intensity of this receptor in the LC of immunodeficient mice (nude and scid) when compared to the wild type ($p < 0.05$). The evaluation of mRNA indicated that, when compared to the baseline (wild type), the androgen receptor levels were 25-fold higher for both immunodeficient mice strains.

The LC cytoplasmic localization of the steroidogenic enzymes 3BHSD (Fig. 2) and aromatase (Fig. 3) was conserved among strains. However, the labeling levels of 3BHSD, as demonstrated by the evaluation of pixel intensity, were higher in nude mice whereas aromatase was equally expressed among strains. A similar pattern was observed from qPCR analyses. 3BHSD mRNA levels were about 25-fold and 50-fold higher in scid and nude mice, respectively. In addition, an increase of approximately 15-fold in aromatase mRNA levels was observed in nude testis when compared to the wild type. On the other hand, the aromatase mRNA levels were similar between scid and wild-type mice.

Foxn1 expression was observed specifically in LC regardless of mice strains (Fig. 4). However, the intracellular distribution of this protein was found to be different, depending on the strain; hence, in wild-type and scid mice, Foxn1 presented both cytoplasmic and nuclear localization, whereas in nude mice, the nuclear labeling was rarely observed. Regarding

Table 4 Cell counts and ratios per seminiferous tubule cross-section at stage VII of the seminiferous epithelium cycle in BALB/c wild type, nude and scid mice (mean ± SEM)

	Wild type	Nude	scid
Sertoli cell (SC) nucleoli	6 ± 0.2^{a}	7.2 ± 0.3^{b}	8.1 ± 0.4^{b}
Type A spermatogonia	1.4 ± 0.1^{a}	1.2 ± 0.1^{b}	1.9 ± 0.1^{c}
Pre-leptotene/leptotene spermatocytes	30 ± 1^{a}	25 ± 1^{b}	30 ± 1^{a}
Pachytene spermatocytes (P)	27 ± 1	28 ± 1	30 ± 1
Round spermatids (R)	63 ± 2	69 ± 4	62 ± 2
Sertoli cell efficiency (R/SC)	10.5 ± 0.2^{a}	9.8 ± 0.5^{a}	7.9 ± 0.5^{b}
Meiotic index (R/P)	2.3 ± 0.004^{a}	2.5 ± 0.1^{a}	2.1 ± 0.04^{b}
Sertoli cell per testis (× 10^6)	3.5 ± 0.1^{a}	2.8 ± 0.2^{a}	4.3 ± 0.3^{b}
Sertoli cell per g of testis (× 10^6)	35 ± 1^{a}	35 ± 2^{a}	51 ± 3^{b}
Daily sperm production per testis (× 10^6)	4.1 ± 0.2^{a}	3.1 ± 0.3^{b}	3.8 ± 0.3^{ab}
Daily sperm production per g of testis (× 10^6)	41 ± 1^{ab}	38 ± 2^{a}	44 ± 2^{b}

Different letters in the same line represent significant statistical difference ($p < 0.05$)

Table 5 Leydig cell parameters in BALB/c wild-type, nude and scid mice (mean ± SEM)

	Wild type	Nude	scid
Nuclear diameter (μm)	7.6 ± 0.1^{a}	6.6 ± 0.1^{b}	7.3 ± 0.1^{a}
Leydig cell individual volume (μm^3)	1444 ± 99^{a}	619 ± 63^{b}	967 ± 43^{c}
Nuclear volume (μm^3)	228 ± 5^{a}	155 ± 8^{b}	207 ± 10^{ab}
Cytoplasmic volume (μm^3)	1216 ± 95^{a}	465 ± 57^{b}	760 ± 35^{c}
Leydig cell number per testis ($\times 10^6$)	2.8 ± 0.4^{a}	9.5 ± 1.1^{b}	7.6 ± 0.2^{c}
Leydig cell number per g of testis ($\times 10^6$)	28.7 ± 4^{a}	121.9 ± 14^{b}	92.3 ± 7^{c}

Different letters in the same line represent significant statistical difference ($p < 0.05$)

DNA-PKc, its expression followed a cytoplasmic distribution in both LC and SC, in wild-type, nude and scid mice (Fig. 4).

Discussion

Although nude and scid mice are important experimental models, there are few reports in the literature regarding their reproductive biology. Therefore, analysis of their testicular structure and function is highly relevant. We comparatively evaluated several important testis morphofunctional parameters in sexually mature nude, scid and wild-type mice. Our main findings strongly suggest that the *Foxn1* gene may be involved in testis endocrine regulation, since substantial differences were observed in nude mice regarding LC, such as number and size, as well as the expression of steroidogenic enzymes. As related to scid mice, the results indicate a relevant role for the *Prkdc* gene in SC and germ cells, as significant increases were observed on SC number and daily sperm production.

It is noteworthy that both mutated genotypes did not induce alterations in testicular cytoarchitecture, since the basic structure of the seminiferous epithelium was preserved. Despite that, differences were observed in several histomorphometric parameters. Interestingly, even though they do not have an increase in Sertoli and germ cell numbers, nude mice

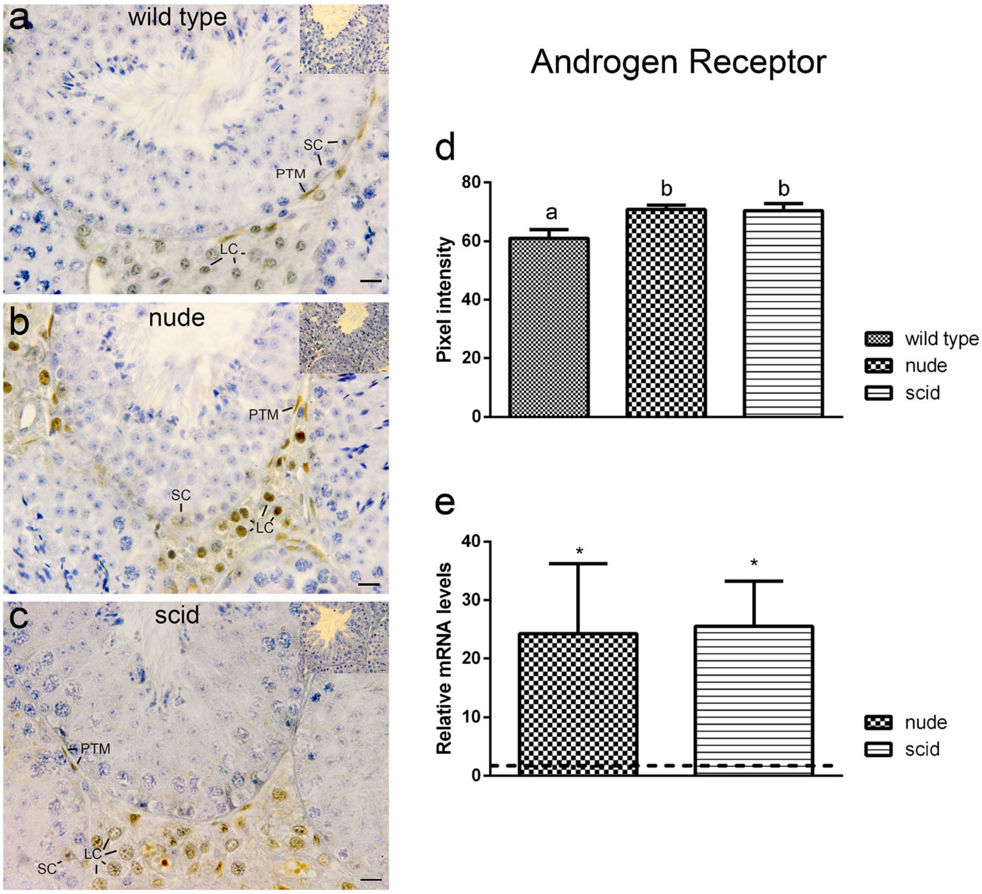

Fig. 1 Androgen receptor expression. Immunolabeling in the Leydig, peritubular myoid and Sertoli cell nucleus in BALB/c wild-type (**a**), nude (**b**) and scid (**c**) mice. Inserts show the negative control. **d** Pixel intensity quantification. **e** Gene expression by qPCR. The dashed line in **e** represents the value of 1, determined for the wild type, and the columns refer to the relative amount of mRNA in the two groups evaluated. LC Leydig cell; PTM peritubular myoid cell; SC Sertoli cell. Different letters and asterisks represent significant statistical difference ($p < 0.05$). Bar = 14 μm

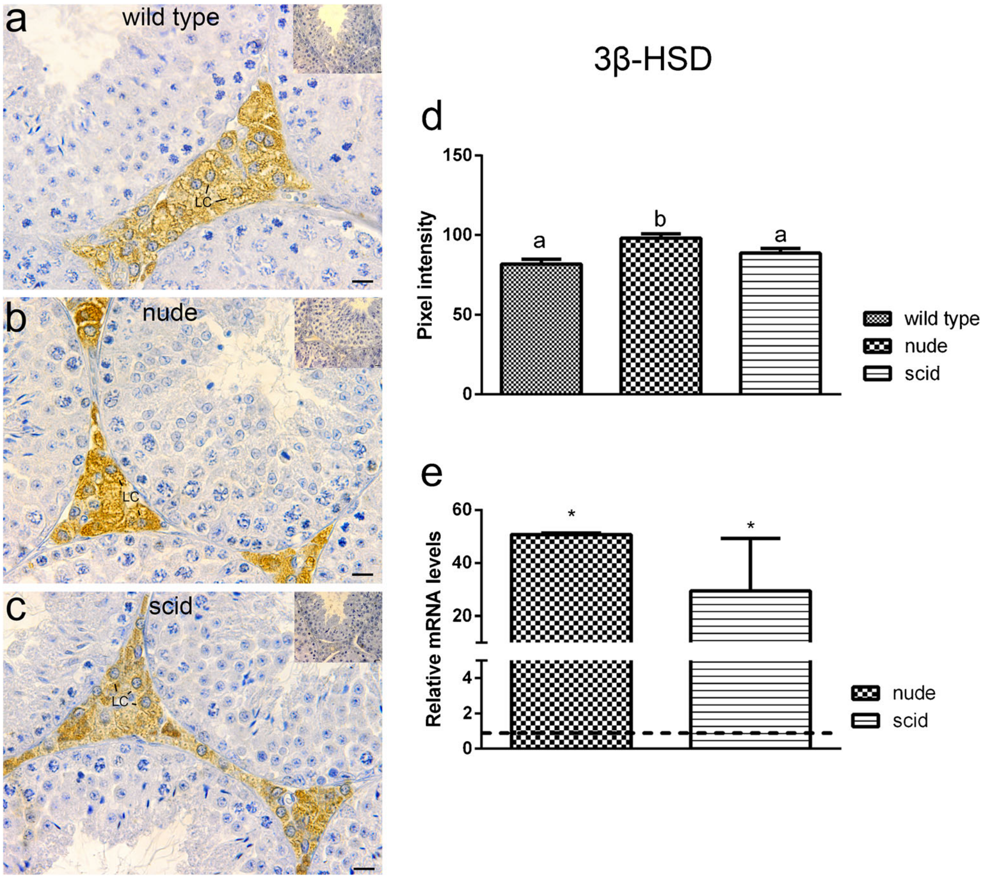

Fig. 2 3β-HSD expression. Immunolabeling in the Leydig cell cytoplasm in BALB/c wild-type (**a**), nude (**b**) and scid (**c**) mice. Inserts show the negative control. **d** Pixel intensity quantification. **e** Gene expression by qPCR. The dashed line in **e** represents the value of 1, determined for the wild type and the columns refer to the relative amount of mRNA in the two groups evaluated. LC Leydig cell. Different letters and asterisks represent significant statistical difference ($p < 0.05$). Bar = 14 μm

showed a higher tubular diameter and a taller seminiferous epithelium height. Although these are related parameters, a decrease in the amount of cells does not necessarily result in a lower epithelium height. This is a very complex and intricate issue that surely deserves further investigation using other methodologies. For instance, Gholami et al. (2015) considered that in some particular conditions, disordered arrangements in the cells or structural adjustments may compensate the epithelium height by increasing the distance between cells.

Furthermore, some differences were also observed in the absolute volume and volume density of several parameters. In the immunodeficient strains, the volume of seminiferous tubules was lower than that in the wild type, while the proportion of the intertubular compartment was increased, mainly due to the higher LC occupancy. In fact, many interesting results were observed for those cells, especially in nude mice. So, since LCs have a smaller individual volume, it seems that their increased total number may be a compensatory mechanism to ensure normal androgen levels and therefore maintain homeostasis. Corroborating these data, a similar LC pattern was also observed in iNOS-deficient mice (Auharek et al. 2011). In this regard, it was important to evaluate the function of these steroidogenic cells, especially because it is already known that testosterone levels are reduced in adult nude mice (Rebar et al. 1982).

Nevertheless, in the present study, we found that, in comparison to the wild type, LC from both immunodeficient strains presented stronger labeling and higher mRNA levels of androgen receptor. It is already documented in the literature that castrated rats have increased androgen receptor mRNA levels as a response to lower levels of circulating testosterone (Tan et al. 1988). Therefore, the same type of receptor upregulation could be happening as a compensatory mechanism, once nude mice have a lower level of circulating androgens, leading to a higher expression of its receptor. Furthermore, some studies already showed that LH is essential for the expression of the P450c17 steroidogenic enzyme but not for 3BHSD (Keeney et al. 1988). Since *Foxn1* mutant mice have lower gonadotropin levels (Rebar et al. 1982), the higher expression of 3BHSD may indicate an attempt to compensate lower levels of LH, in order to better use the available substrate (pregnenolone), once its synthesis could be downregulated. Another important steroidogenic enzyme is aromatase, which converts androgen into estrogen (Genissel et al. 2001). Once there are less androgens in nude mice (Rebar et al. 1982), the increase in aromatase mRNA levels in this strain also suggests a compensatory mechanism to ensure suitable

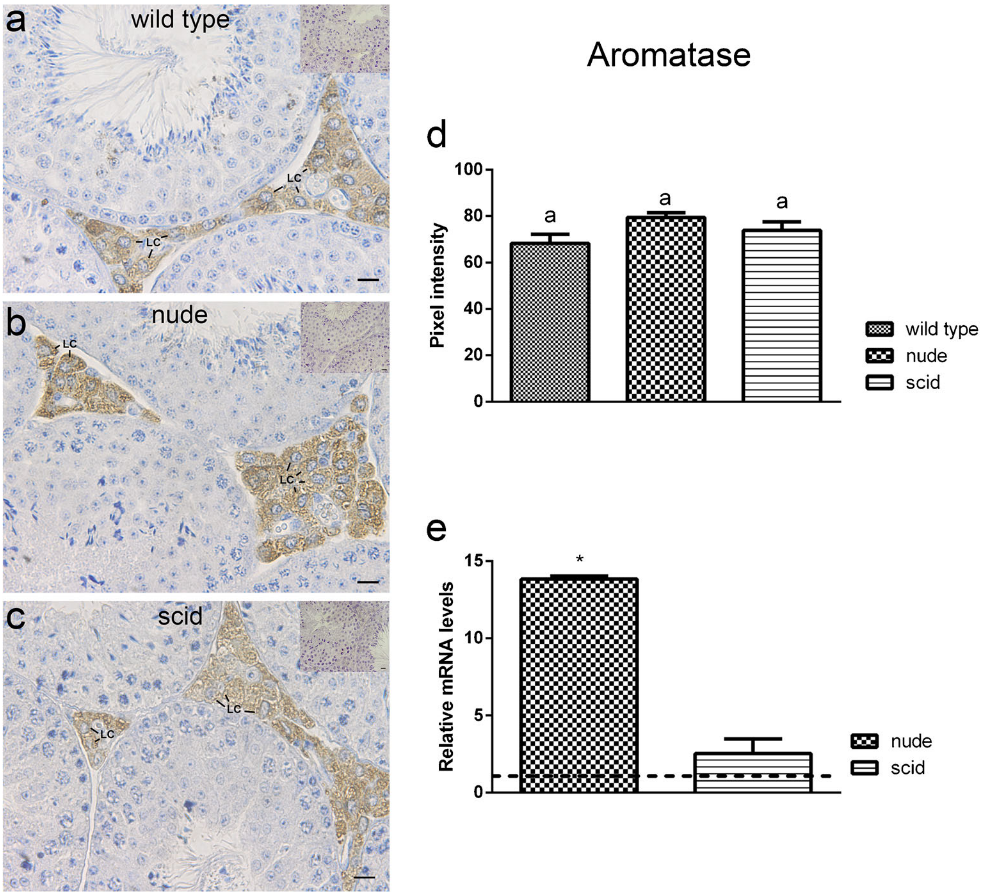

Fig. 3 Aromatase expression. Immunolabeling in the Leydig cell cytoplasm in BALB/c wild-type (**a**), nude (**b**) and scid (**c**) mice. Inserts show the negative control. **d** Pixel intensity quantification. **e** Gene expression by qPCR. The dashed line in **e** represents the value of 1, determined for the wild type and the columns refer to the relative amount of mRNA in the two groups evaluated. LC Leydig cell. Different letters and asterisks represent significant statistical difference ($p < 0.05$). Bar = 14 μm

estrogen levels, in order to maintain testicular physiological function.

Thus, the evaluation of localization and grade of protein expression in Leydig cell was enabled, once immunohistochemistry preserves the tissue cytoarchitecture. Therefore, the measurement of pixel intensity, observed for many authors (Dornas et al. 2007, 2008; Oliveira et al. 2013) as a suitable methodology for evaluating protein occurrence, was considered in the present study as a qPCR complementary tool that provided some important information regarding differential expression of steroidogenic enzymes and androgen receptor across the strains.

Spermatogenesis requires a balance between proliferation and apoptosis, which regulates the number of germ cells supported by each SC, ensuring the homeostasis of sperm production. The highest germ cell loss in meiosis was found in the scid mice and it is consistent with previous reports describing more apoptosis in pachytene spermatocytes at stage IV in mice carrying the *Prkdc* gene mutation (Hamer et al. 2003; De Rooij and De Boer 2003). Consequently, an important parameter that ultimately defines daily sperm production, the SC efficiency, was found to be reduced in scid mice (7.9 round spermatids per SC), a value comparable to the less efficient species already investigated, such as dog and marmoset (Lara et al. 2018).

In rodents, SC proliferation occurs during fetal and postnatal periods and is mainly regulated not only by FSH and androgens but also by the insulin family of growth factors, activin and cytokines (Desjardins and Ewing 1993; Meachem et al. 2005; Scott et al. 2008; Lucas et al. 2014; Meroni et al. 2019). Interestingly, in the Sertoli cell–selective androgen receptor knockout (SCARKO) mouse, the final number of Sertoli cells is unaltered, while the androgen receptor knockout (ARKO) mouse exhibits a progressive reduction in SC number/testis (Tan et al. 2005). This happens because androgens do not modulate SC proliferation via direct action on SC, since SC starts expressing androgen receptor when they become mature and stop proliferating. Therefore, androgen receptor expression in other testicular cell types (especially peritubular myoid cells (PTMCs)) is considered an important mediator for the stimulatory effect of testosterone on Sertoli cell proliferation (Buzzard et al. 2003; Tan et al. 2005).

The higher SC number observed in scid mice may suggest a higher proliferative activity or an extension of its proliferative period. Although there are no reports concerning the hormonal profile of scid mice during postnatal development, our

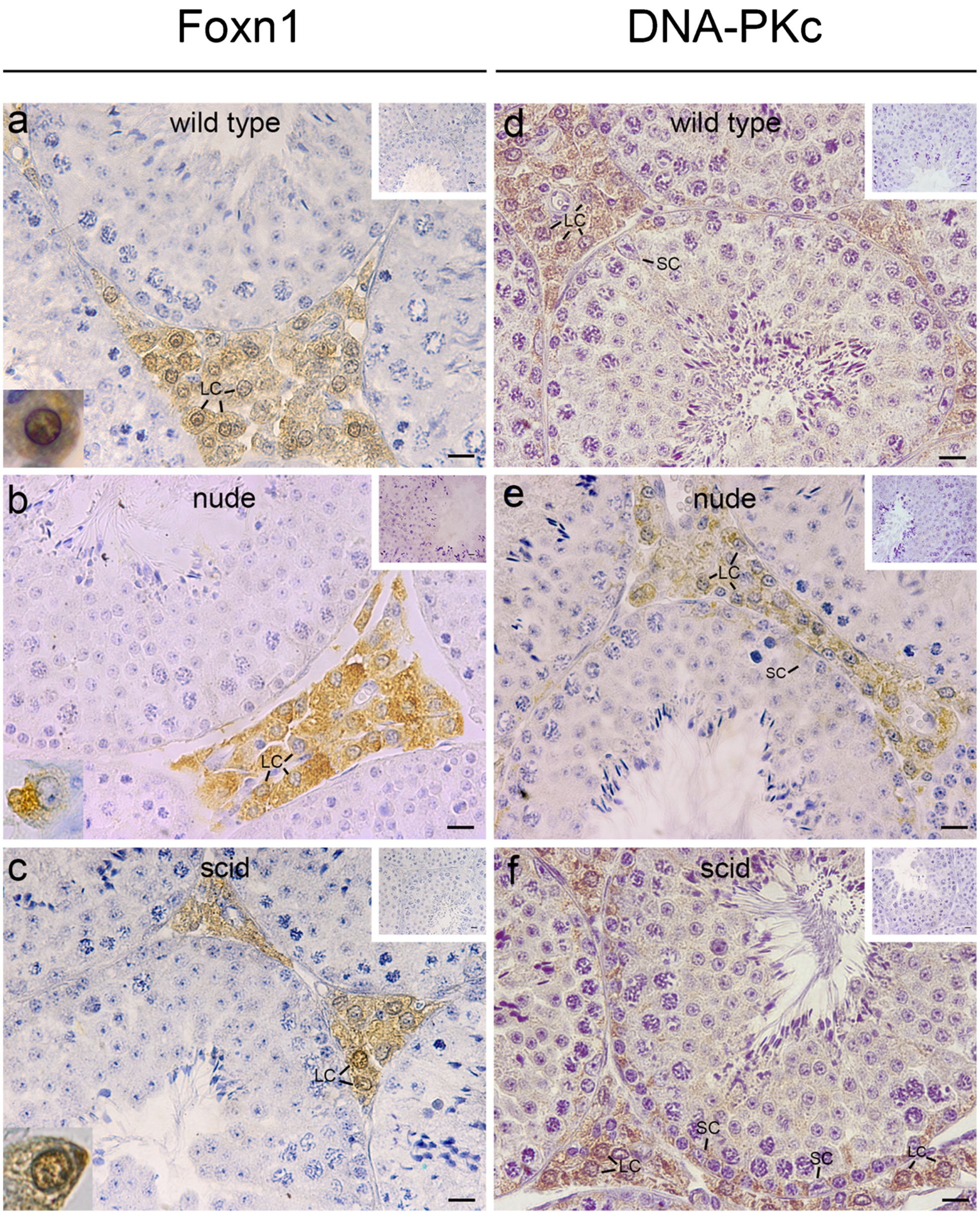

Fig. 4 Distribution of Foxn1 and DNA-PKc in the testis. Expression of the transcription factor Foxn1 in the testis of BALB/c wild type (**a**), nude (**b**) and scid (**c**) mice. **a**, **c** The expression of the protein in the cytoplasm and nucleus of the Leydig cells. **b** The nuclear labeling is absent in the Leydig cells. Distribution of the protein DNA-PKc in the testis of BALB/c wild-type (**d**), nude (**e**) and scid (**f**) mice. Note the cytoplasmic labeling in the Leydig and Sertoli cells. LC Leydig cell; SC Sertoli cell. Bar = 14 μm

indirect evaluation of androgen action by androgen receptor and 3BHSD analyses indicated a higher expression of these proteins in the testis of adult scid mice. Therefore, it is reasonable to hypothesize that androgens' indirect effect, possibly exerted through the secretion of paracrine factors (such as activin A, produced by PTMC), stimulates SC proliferation in scid mice. Due to the observed increase in SC number, total seminiferous tubule length and daily sperm production, which are highly correlated parameters, the scid mice showed the highest spermatogenic efficiency (daily sperm production per gram of testis) among the three groups investigated, despite its lowest SC efficiency.

The transcription factor Foxn1 is translocated to the cell nucleus after phosphorylation, where it regulates the expression of several genes (Mecklenburg et al. 2005). In the present study, we observed that Foxn1 was equally expressed in the LC cytoplasmic compartment across the strains, whereas its nuclear expression was rarely observed in nude mice. The difference regarding intracellular distribution of Foxn1 protein is probably explained by the fact that nude mice mutation generates a premature stop codon, producing an unstable inactive protein that lacks the DNA binding domain (Nehls et al. 1994; Brissette et al. 1996). Therefore, although still producing the protein, as observed by its presence in the LC cytoplasm, Foxn1 expression was rarely seen in the nucleus, being inactive in nude mice. In this context, the cytoplasmatic/nuclear distribution of the Foxn1 transcription factor in the wild-type LC strongly suggests its participation in the genetic regulation of the function of these cells, possibly in the steroidogenic pathway. This type of steroidogenic regulation is already observed for another protein of the forkhead family, Foxl2, which is a transcription factor involved in the modulation of the expression of steroidogenic acute regulatory protein (*StAR*) and aromatase (*CYP19A1*) genes (Pisarska et al. 2004; Pannetier et al. 2006).

Regarding the DNA-PK enzyme, its presence was already described in the germ cell nucleus and in the cytoplasm of SC and LC (Hamer et al. 2003). Therefore, once this protein was observed in the cytoplasm of SC and LC in the present study, our results indicate the involvement of these somatic cells in the synthesis of the catalytic subunit of DNA-PK repair enzyme. The *Prkdc* gene mutation also leads to a premature stop codon, synthesizing an unstable protein that accumulates in the cytoplasm (Blunt et al. 1996), which explains the expression of this protein also in scid mice testis.

It is important to mention that even though nude and scid mice strains share an immunodeficient phenotype, our results indicate that testicular alterations in these mice are probably more related to their genotypes than to the immunodeficiency itself. Corroborating that, we observed that many parameters differed between nude and scid mice, which indicates that several and different mechanisms led to the distinct observed testicular alterations. Moreover, suggesting a particular role for these proteins in testis function, we identified the expression of DNA-PKc and Foxn1 in the testis.

Taken together, our present findings provide a better understanding of nude and scid mice adult testis function. For the first time, we showed that Foxn1 and DNA-PKc proteins might play a role in maintaining testis physiology. Considering these quite relevant results and, in order to better understand the involvement of *Foxn1* in testis function, we are currently investigating the role of this transcription factor during postnatal testis development, particularly focusing on LC. In summary, the immunodeficient nude and scid mice have unique testicular characteristics that make them adequate models to investigate the testis regulatory mechanisms, in particular the pathways involved in the control of SC and LC proliferation and function in mammals.

Acknowledgments Technical assistance from Mara Lívia dos Santos is highly appreciated.

Funding information This work was supported by the Brazilian National Council for Scientific and Technological Development (CNPq), the Foundation for Research Support of Minas Gerais (FAPEMIG) and the Coordination for the Improvement of Higher Education Personnel (CAPES).

Compliance with ethical standards

Conflict of interest The authors declare that they have no conflict of interest.

Ethical approval All procedures performed in studies involving animals were in accordance with the ethical standards of the institution at which the studies were conducted (Ethics Committee in Animal Experimentation of the Federal University of Minas Gerais—CETEA/UFMG—Protocol no. 123/2013).

References

Abercrombie M (1946) Estimation of nuclear populations from microtome sections. Anat Rec 94:238–248

Amann RP, Almquist JO (1962) Reproductive capacity of dairy bulls. Direct and indirect measurement of testicular sperm production. J Dairy Sci 45:774–781

Attal J, Courot M (1963) Development testiculaire et etablissement de la spermatogenese chez le taureau. Ann Biol Anim Biochem Biophys 8:219–241

Auharek SA, Avelar GF, Lara NL, Sharpe RM, França LR (2011) Sertoli cell numbers and spermatogenic efficiency are increased in inducible nitric oxide synthase mutant mice. Int J Androl. https://doi.org/10.1111/j.1365-2605.2011.01209.x

Blunt T, Gell D, Fox M, Taccioli GE, Lehmann AR, Jackson SP, Jeggo PA (1996) Identification of a nonsense mutation in the carboxyl-terminal region of DNA-dependent protein kinase catalytic subunit in the scid mouse. Proc Natl Acad Sci 93:10285–10290

Brissette JL, Li J, Kamimura J, Lee D, Dotto GP (1996) The product of the mouse nude locus, Whn, regulates the balance between epithelial cell growth and differentiation. Genes Dev 10:2212–2221

Buzzard JJ, Farnworth PG, De Kretser DM, O'Connor AE, Wreford NG, Morrison JR (2003) Proliferative phase sertoli cells display a developmentally regulated response to activin in vitro. Endocrinology. https://doi.org/10.1210/en.2002-220595

Byrd LG (1993) Regional localization of the nu mutation on mouse chromosome 11. Immunogenetics 37:157–159

De Rooij DG, De Boer P (2003) Specific arrest of spermatogenesis in genetically modified and mutant mice. Cytogenet Genome Res. https://doi.org/10.1159/000076812

Desjardins C, Ewing LL (1993) Cell and molecular biology of the testis, 1st edn. Oxford University Press, New York

Dornas RA, Oliveira AG, Kalapothakis E, Hess RA, Mahecha GA, Oliveira CA (2007) Distribution of vitamin D3 receptor in the epididymal region of roosters (Gallus domesticus) is cell and segment specific. Gen Comp Endocrinol. https://doi.org/10.1016/j.ygcen.2006.10.010

Dornas RA, Oliveira AG, Dias MO, Mahecha GA, Oliveira CA (2008) Comparative expression of androgen receptor in the testis and epididymal region of roosters (Gallus domesticus) and drakes (Anas platyrhynchos). Gen Comp Endocrinol. https://doi.org/10.1016/j.ygcen.2007.08.010

Dorst VJ, Sajonski H (1974) Morphometrische Untersuchunhen am Tubulussys-tem des Schweinehodens wahrend der postnatalen Entwicklug. Monaths Vet Med 29:650–652

Franca LR. (1992) Daily sperm production in Piau boars estimated from Sertoli cell population and Sertoli cell index. In: Proceedings of the 12th International Congress on animal reproduction and artificial insemination, vol. 4. The hague: The ICAR (ed. SJ Dieleman), pp. 1716–1718. Elsevier Science, The Hague

Genissel C, Levallet J, Carreau S (2001) Regulation of cytochrome P450 aromatase gene expression in adult rat Leydig cells: comparison with estradiol production. J Endocrinol 168:95–105

Gholami S, Ansari-lari M, Khalili L (2015) Histologic and histomorphometric changes of testis following oral exposure to methyl tertiary-butyl ether in adult rat. Iran J Vet Res 16(3):288–292

Goertz MJ, Wu Z, Gallardo TD, Hamra FK, Castrillon DH (2011) Foxo1 is required in mouse spermatogonial stem cells for their maintenance and the initiation of spermatogenesis. J Clin Invest. https://doi.org/10.1172/JCI57984

Hamer G, Roepers-Gajadien HL, Van Duyn-Goedhart A, Gademan IS, Kal HB, Van Buul PP, Ashley T, De Rooij DG (2003) Function of DNA-protein kinase catalytic subunit during the early meiotic prophase without Ku70 and Ku86. Biol Reprod 68:717–721

Hochereau-de Reviers MT, Lincoln GA (1978) Seasonal variation in the histology of the testis of the red deer, Cervus elephus. J Reprod Fertil 54:209–213

Jasurda JS, Jung DO, Froeter ED, Schwartz DB, Hopkins TD, Farris CL, McGee S, Narayan P, Ellsworth BS (2014) The forkhead transcription factor, FOXP3: a critical role in male fertility in mice. Biol Reprod. https://doi.org/10.1095/biolreprod.113.112375

Justice NJ, Blount AL, Pelosi E, Schlessinger D, Vale W, Bilezikjian LM (2011) Impaired FSHβ expression in the pituitaries of Foxl2 mutant animals. Mol Endocrinol. https://doi.org/10.1210/me.2011-0093

Keeney DS, Mendis-Handagama SMLC, Zirkin BR, Ewing LL (1988) Effect of long term deprivation of luteinizing hormone on Leydig cell volume, Leydig cell number and steroidogenic capacity of the rat testis. Endocrinology. https://doi.org/10.1210/endo-123-6-2906

Lara NLM, Costa GMJ, Avelar GF, Lacerda SMSN, Hess RA, França LR (2018) Testis physiology—overview and histology. In: Skinner MK (ed) Encyclopedia of reproduction. Academic, Elsevier, pp 105–116

Lees-Miller SP, Meek K (2003) Repair of DNA double strand breaks by non-homologous end joining. Biochimie 85:1161–1173

Lucas TF, Nascimento AR, Pisolato R, Pimenta MT, Lazari MF, Porto CS (2014) Receptors and signaling pathways involved in proliferation and differentiation of Sertoli cells. Spermatogenesis. https://doi.org/10.4161/spmg.28138

Meachem SJ, Ruwanpura SM, Ziolkowski J, Ague JM, Skinner MK, Loveland KL (2005) Developmentally distinct in vivo effects of FSH on proliferation and apoptosis during testis maturation. J Endocrinol. https://doi.org/10.1677/joe.1.06121

Mecklenburg L, Tychsen B, Paus R (2005) Learning from nudity: lessons from the nude phenotype. Exp Dermatol. https://doi.org/10.1111/j.1600-0625.2005.00362.x

Meroni SB, Galardo MN, Rindone G, Gorga A, Riera MF, Cigorraga SB (2019) Molecular mechanisms and signaling pathways involved in Sertoli cell proliferation. Front Endocrinol. https://doi.org/10.3389/fendo.2019.00224

Morais RDVS, Crespo D, Nóbrega RH, Lemos MS, van de Kant HJG, de França LR, Male R, Bogerd J, Schulz RW (2017) Antagonistic regulation of spermatogonial differentiation in zebrafish (Danio rerio) by Igf3 and Amh. Mol Cell Endocrinol. https://doi.org/10.1016/j.mce.2017.06.017

Nehls M, Pfeifer D, Schorpp M, Hedrich H, Boehm T (1994) New member of the winged-helix protein family disrupted in mouse and rat nude mutations. Nature. https://doi.org/10.1038/372103a0

Oliveira RL, Campolina-Silva GH, Nogueira JC, Mahecha GA, Oliveira CA (2013) Differential expression and seasonal variation on aquaporins 1 and 9 in the male genital system of big fruit-eating bat Artibeus lituratus. https://doi.org/10.1016/j.ygcen.2013.02.041

Pannetier M, Fabre S, Batista F, Kocer A, Renault L, Jolivet G, Mandon-Pépin B, Cotinot C, Veitia R, Pailhoux E (2006) FOXL2 activates P450 aromatase gene transcription: towards a better characterization of the early steps of mammalian ovarian development. J Mol Endocrinol. https://doi.org/10.1677/jme.1.01947

Pisarska MD, Bae J, Klein C, Hsueh AJ (2004) Forkhead l2 is expressed in the ovary and represses the promoter activity of the steroidogenic acute regulatory gene. Endocrinology. https://doi.org/10.1210/en.2003-1141

Rebar RW, Morandini IC, Petze JE, Erickson GF (1982) Hormonal basis of reproductive defects in athymic mice: reduced gonadotropins and testosterone in males. Biol Reprod 27:1267–1276

Sampaio IMB (2002) Statistic applied to animal experimentation. 2nd. FEPMVZ, Belo Horizonte

Scott HM, Hutchison GR, Jobling MS, McKinnell C, Drake AJ, Sharpe RM (2008) Relationship between androgen action in the “male programming window,” fetal sertoli cell number, and adult testis size in the rat. Endocrinology. https://doi.org/10.1210/en.2008-0413

Skarra DV, Arriola DJ, Benson CA, Thackray VG (2013) Forkhead box O1 is a repressor of basal and GnRH-induced Fshb transcription in gonadotropes. Mol Endocrinol. https://doi.org/10.1210/me.2013-1185

Sprando RL, Santulli R, Awoniyi CA, Ewing LL, Zirkin BR (1990) Does ethane 1,2-dimethanesulphonate (EDS) have a direct cytotoxic effect on the seminiferous epithelium of the rat testis? J Androl 11:344–352

Tan J, Joseph DR, Quarmby VE, Lubahn DB, Sar M, French FS, Wilson EM (1988) The rat androgen receptor: primary structure, autoregulation of its messenger ribonucleic acid, and immunocytochemical localization of the receptor protein. Mol Endocrinol. https://doi.org/10.1210/mend-2-12-1276

Tan KA, De Gendt K, Atanassova N, Walker M, Sharpe RM, Saunders PT, Denolet E, Verhoeven G (2005) The role of androgens in sertoli cell proliferation and functional maturation: studies in mice with total or Sertoli cell-selective ablation of the androgen receptor. Endocrinology. https://doi.org/10.1210/en.2004-1630

Thackray VG (2014) Fox tales: regulation of gonadotropin gene expression by forkhead transcription factors. Mol Cell Endocrinol. https://doi.org/10.1016/j.mce.2013.09.034

Uhlenhaut NH, Treier M (2011) Forkhead transcription factors in ovarian function. Reproduction. https://doi.org/10.1530/REP-11-0092

Publisher's note Springer Nature remains neutral with regard to jurisdictional claims in published maps and institutional affiliations.